ISSN 0006-2979, Biochemistry (Moscow), 2019, Vol. 84, No. 3, pp. 299-309. © Pleiades Publishing, Ltd., 2019.
Published in Russian in Biokhimiya, 2019, Vol. 84, No. 3, pp. 423-435.

A Platform for Studying Neurodegeneration Mechanisms Using Genetically Encoded Biosensors

E. I. Ustyantseva[1,2,3,4], S. P. Medvedev[1,2,3,4], A. S. Vetchinova[5], J. M. Minina[1], S. N. Illarioshkin[5], and S. M. Zakian[1,2,3,4,a]*

[1]*Federal Research Center Institute of Cytology and Genetics, Siberian Branch of the Russian Academy of Sciences, 630090 Novosibirsk, Russia*
[2]*Institute of Chemical Biology and Fundamental Medicine, Siberian Branch of the Russian Academy of Sciences, 630090 Novosibirsk, Russia*
[3]*Meshalkin National Medical Research Center, Ministry of Health of the Russian Federation, 630055 Novosibirsk, Russia*
[4]*Novosibirsk State University, 630090 Novosibirsk, Russia*
[5]*Research Center of Neurology, 125367 Moscow, Russia*
[a]*e-mail: Zakian@bionet.nsc.ru*

Received October 14, 2018
Revised November 11, 2018
Accepted November 11, 2018

Abstract—Patient-specific induced pluripotent stem cells (iPSCs) capable of differentiation into required cell type are a promising model for studying various pathological processes and development of new therapeutic approaches. However, no conventional strategies for using iPSCs in disease research have been established yet. Genetically encoded biosensors can be used for monitoring messenger molecules, metabolites, and enzyme activity in real time with the following conversion of the registered signals in quantitative data, thus allowing evaluation of the impact of certain molecules on pathology development. In this article, we describe the development of a universal cell-based platform for studying pathological processes associated with amyotrophic lateral sclerosis. For this purpose, we have created a series of plasmid constructs for monitoring endoplasmic reticulum stress, oxidative stress, apoptosis, and Ca^{2+}-dependent hyperexcitability and generated transgenic iPSC line carrying mutation in the superoxide dismutase 1 gene (*SOD1*) and healthy control cell line. Both cell lines have specific transactivator sequence required for doxycycline-controlled transcriptional activation and can be used for a single-step biosensor insertion.

DOI: 10.1134/S000629791903012X

Keywords: induced pluripotent stem cells, biosensors, CRISPR/Cas9

Induced pluripotency was discovered relatively recently, in 2006, when the first protocol for the generation of pluripotent stem cells from adult mouse fibroblasts was published [1]. The cells were generated by ectopic expression of four genes – *Oct4*, *Sox2*, *Klf4*, and *c-Myc* – and were named induced pluripotent stem cells (iPSCs). Human iPSCs were discovered just one year after [2] and immediately came into notice as a model system for studying various physiological and pathological processes. Two major features – self-renewal and ability to differentiate into multiple cell types – have made iPSCs highly attractive for biomedical studies, because iPSCs they can be obtained from a patient suffering from a particular disease in a harmless way, as well as used for both research and disease treatment.

From the moment the first human iPSCs were obtained, a number of disease models have been developed using patient-specific iPSCs [3, 4], most of them being models of monogenic hereditary diseases, although cell models of sporadic or multifactorial disorders (e.g., Alzheimer's disease) also exist [5]. It should be noted that cells derived from patient-specific iPSCs recapitulate disease phenotype, proving the suitability of this kind of model system for research [6-9].

Abbreviations: ALS, amyotrophic lateral sclerosis; CRISPR/Cas9, clustered regularly interspaced short palindromic repeats/CRISPR-associated; EB, embryonic body; ER, endoplasmic reticulum; iPSCs, induced pluripotent stem cells; MBCs, mononuclear blood cells; PBS, phosphate buffered saline; SOD1, superoxide dismutase 1.

* To whom correspondence should be addressed.

Table 1. Fragments used for the construction of donor plasmids

Name	Fragment content	Fragment source and/or PCR primers, 5′-3′
1	2	3
sgAAVS1-F	–	CACCGGTCACCAATCCTGTCCCTAG
sgAAVS1-R	–	AAACCTAGGGACAGGATTGGTGACC
HM-MCS-U	multiple cloning site	CGGCGCGCCCTTAAGGTTAACACGCGTGGCGCGCCA
HM-MCS-L	multiple cloning site	CTAGTGGCGCGCCACGCGTGTTAACCTTAAGGGCGC-GCCGGTAC
HA-R-CMV	right homology arm to *AAVS1* locus (HA-R), TRE-minCMV promoter	Puro-Cas9 donor (Addgene #58409, [38]), ACGCGTGGCGATCTGACGGTTCACT, ACTAGTAGAGCAGAGCCAGGAACC
Cas9-HF1	SpCas9-HF1, SV40 NLS, 3xFLAG epitope, bGHpoly(A)	VP12 (Addgene #72247, [39]), ACGCGTGCCACCATGGATAAAAAG, CTTAAGCCATAGAGCCCACCGCA
SV40poly(A)	SV40poly(A)	pcDNA 3.1/Hygro (–), GCAACCGGTACGAGATTTCGATTCCACCG, CAGCTTAAGTAAGATACATTGATGAGTTTG
HA-L-Puro	left homology arm to *AAVS1* locus (HA-L), puromycin resistance sequence, bGHpoly(A)	Puro-Cas9 donor (Addgene #58409, [38]), GGTACCTGCTTTCTCTGACCAGCATT, CTTAAGCCATAGAGCCCACCGCAT
XBP1	XBP1 fragment, containing stress-response element	cDNA synthesized by qPCR from RNA isolated from human brain tissue, GCGCGGTGCGTAGTCTGGAGC, GGTATATATGTGGTCAAAACG
XBP1ΔDBD, XBP1_indel	XBP1, spliced/unspliced variants	pGEM-T-Easy_XBP1, CAAGCTAGCGCCACCATGGACTA-CAAAGACGATGACGACAAGGAGAAAACTCATGGCCTTG-TAGTTGAG, AATGGTACCCCCTAAGTCAATACCGCCAGAATCC
TagRFP	TagRFP without start codon	pTagRFP-N (Evrogen, Russia), GTCGGTACCGTGTCTAAGGGCGAAGAGCTG, GCGCTTAAGTTAATTAAGCTTGTGCCCCA
XBP1-TagRFP, XBP1-TagRFP_indel	XBP1, TagRFP	pCMV-XBP1-TagRFP, pCMV-XBP1-TagRFP_indel, CTGACGCGTGCCACCATGGACTACAAAG, CGCACCGGTTCAATTAAGTTTGTGCCCCA
Cyto-Grx1-roGFP2	Grx1-roGFP2	pLPCX cyto Grx1-roGFP2 (Addgene #64975 [22]), ACCACGCGTGCCACCATGGCTCAAGAGTTTGTGAAC, TTTACCGGTTTACTTGTACAGCTCGTCC
Mito-Grx1-roGFP2	Grx1-roGFP2, signal peptide (ATP synthase subunit 9)	pLPCX mito Grx1-roGFP2 (Addgene #64977, [22]), GACACGCGTGCCACCATGGCCTCCACTCGTGTCCTC, TTTACCGGTTTACTTGTACAGCTCGTCC
Cyto-roGFP2-Orp1	roGFP2-Orp1	pLPCX roGFP2-Orp1 (Addgene #64991, [40]), GACACGCGTGCCACCATGGTGAGCAAGGGCGAGGAG, TTTACCGGTCTATTCCACCTCTTTCAAAAG
Mito-roGFP2-Orp1	roGFP2-Orp1, signal peptide (ATP synthase subunit 9)	pLPCX mito roGFP2-Orp1 (Addgene #64992, [40]), GACACGCGTGCCACCATGGCCTCCACTCGTGTCC, TTTACCGGTCTATTCCACCTCTTTCAAAAG

Table 1 (Contd.)

1	2	3
Casper3-BG	BFP, TagGFP2, caspase 3 site	pCasper3-BG (Evrogen), CCAACGCGTGCCACCATGAGCGAGCTGAT, CGCCTTAAGATACATTGATGAGTTTGGAC
Casper3-GR	TagGFP2, RFP, caspase 3 site	pCasper3-GR (Evrogen), CCAACGCGTGCCACCATGGTGAGCGAGCT, CGCCTTAAGATACATTGATGAGTTTGGAC
GCaMP6f	calmodulin_fast, GFP, calmodulin-binding peptide	pAAV.Syn.GCaMP6f.WPRE.SV40 (Addgene #100837, [29]), GATACGCGTGCCACCATGGGTTCTCATCATC, GATACCGGTTCACTTCGCTGTCATCATTTGTAC
GCaMP6m	calmodulin_medium, GFP, calmodulin-binding peptide	pAAV.Syn.GCaMP6m.WPRE.SV40 (Addgene #100841,[29]), GATACGCGTGCCACCATGGGTTCTCATCATC, GATACCGGTTCACTTCGCTGTCATCATTTGTAC
GCaMP6s	calmodulin_slow, GFP, calmodulin-binding peptide	pAAV.Syn.GCaMP6s.WPRE.SV40 (Addgene #100843, [29]), GATACGCGTGCCACCATGGGTTCTCATCATC, GATACCGGTTCACTTCGCTGTCATCATTTGTAC

The use of iPSCs for studying neurodegeneration is of particular interest, since neurodegenerative disorders have unclear etiology and complex pathogenesis and, as a result, lack proper and efficient treatment options preventing neuronal death. Amyotrophic lateral sclerosis (ALS) is one of neurodegenerative disorders characterized by the death of both lower and upper motor neurons [10]. Clinical manifestations of ALS include paralysis of skeletal muscles and the diaphragm resulting in the respiratory failure as the most common cause of death [11]. However, some ALS features such, as age of onset, progression rate, presence/absence of cognitive decline, and others can vary from patient to patient making ALS one of the most heterogeneous disease among neurodegenerative disorders. Neither etiology nor pathogenic mechanisms of ALS have been elucidated so far [12-14]. Up to 10% of ALS cases are familial, the list of causative genes including more than 100 names [15]. These genes often encode proteins involved in basic cellular processes, such as protein and RNA homeostasis, cellular transport, and utilization of reactive oxygen species [16, 17].

Experiments in ALS animal models promote the understanding of general features of ALS progression at the systemic level. They, however, do not allow to investigate pathology development in time – from the onset through early to the advanced disease stages [18, 19]. New technologies for iPSC generation and protocols for iPSC directed differentiation resulted in the creation of a cell-based model system for studying pathological features of motor neurons. However, most such studies are limited to the investigation of gene expression profiles with subsequent association analysis [9] or elucidation of particular metabolic processes [20, 21], thereby failing to facilitate the understanding of the cause-effect relationship between the processes leading to the death of motor neurons in ALS.

Genetically encoded biosensors are widely used for studying various biological processes. They allow to monitor specific signaling molecules, enzymes, and metabolites in solutions, cells, and even animals [22, 23]. The mechanism of biosensor function is based on the ability of certain proteins to change their conformation in response to specific stimuli [24]. These changes induce generation of a reporter signal (fluorescent, luminescent, or electrochemical) that can be registered and evaluated quantitatively. A number of biosensors based on fluorescent proteins have been created and actively used in different cell systems [25, 26], e.g., for registration of different pathological processes typical for neurodegeneration, such as apoptosis, oxidative stress, endoplasmic reticulum (ER) stress, and hyperexcitability [27-29].

MATERIALS AND METHODS

CRISPR/Cas9 plasmid construction. The pX458-AAVS1 plasmid encoding Cas9 and guide RNA for the double-strand break generation in the *AAVS1* locus was constructed based on the pSpCas9(BB)-2A-GFP vector (#48138; Addgene, USA [30]). Two oligonucleotides, sgAAVS1-F and sgAAVS1-R (Table 1), were annealed and inserted into pSpCas9(BB)-2A-GFP using BbsI restriction sites.

Construction of donor plasmids. Donor plasmids containing biosensor sequences, puromycin resistance

sequence, and homology arms to the *AVVS1* locus were generated by ligation of the corresponding PCR fragments into the vectors (Table 1).

The pSpCas9-HF1-donor plasmid was constructed by insertion of five DNA fragments into the pBluescript SK(+) plasmid. Synthetic oligonucleotides HM-MCS-U and HM-MCS-L (Table 1) containing restriction sites for AflII and MluI were annealed and cloned into the pBluescript SK(+) vector using Acc65I and SpeI restriction sites, resulting in the generation of pBluescript SK(+) MCS. The HA-R-CMV fragment was inserted into pBluescript SK(+) MCS by SpeI and MluI restriction endonuclease sites. The Cas9-HF1 fragment was inserted by the MluI and AflII sites. The bGHpolyA polyadenylation signal located between AgeI and AflII restriction sites was replaced by the SV40poly(A) sequence. Finally, the HA-L-Puro fragment was inserted by the Acc65I and AflII sites.

All other donor plasmids were obtained based on pSpCas9-HF1-donor by replacement of the fragment flanked by the MluI and AgeI/AflII cloning sites.

The pXBP1-TagRFP-ERSS donor plasmid was constructed by cloning of the XBP1 fragment into pGEM-T Easy (Promega, USA). The XBP1ΔDBD and XBP1_indel fragments were obtained by PCR using pGEM-T Easy_XBP1 as a template and cloned into pcDNA 3.1/Hygro(−) by the NheI and Acc65I sites. The TagRFP sequence was inserted in the same vector by the Acc65I and AflII sites. The resulting plasmid was used for PCR amplification of the XBP1-TagRFP and XBP1-TagRFP_indel fragments that were inserted in pSpCas9-HF1-donor by the MluI and AgeI sites.

For the generation of pCyto-Grx1-roGFP2-donor and pMito-Grx1-roGFP2-donor plasmids, Cyto-Grx1-roGFP2 and Mito-Grx1-roGFP2 fragments, respectively, were cloned in pSpCas9-HF1-donor by the MluI and AgeI sites. The pCyto-roGFP2-Orp1-donor and pMito-roGFP2-Orp1-donor plasmids were generated by insertion of the Cyto-roGFP2-Orp1 and Mito-roGFP2-Orp1 fragments, respectively, in pSpCas9-HF1-donor by the MluI and AgeI sites.

pCasper3-BG-donor and pCasper3-GR-donor plasmids were obtained by insertion of the Casper3-BG and Casper3-GR fragments, respectively, in pSpCas9-HF1-donor by the MluI and AflII sites.

pAAVS-TRE-CMV-GCaMP6f/m/s plasmids were constructed by insertion of the GCaMP6f, GCaMP6m, and GCaMP6s fragments, respectively, into pSpCas9-HF1-donor by the MluI and AgeI sites.

All generated plasmids were produced in *E. coli* XL10-GOLD Kan^r cells (Agilent, USA). Transformed *E. coli* cells were grown at 30°C. Q5® High-Fidelity DNA Polymerase (New England Biolabs, USA) or Phusion™ Hot Start II High-Fidelity DNA Polymerase (Thermo Fisher Scientific, USA) were used for all PCR reactions; restriction endonucleases were from New England Biolabs, Promega and Sibenzyme (Russia); T4 DNA ligase was from Thermo Fisher Scientific. The accuracy of cloning was verified by Sanger sequencing.

Cell culturing and reprogramming. Mononuclear blood cells (MBCs) with the D90A mutation in superoxide dismutase (SOD1) gene were obtained from an ALS patient at the Research Center of Neurology (Moscow) and isolated by Ficoll gradient centrifugation (1.077 g/ml; Biolot, Russia). MBCs were thawed 5 days prior to reprogramming and cultured according to the published protocol [31] at 37°C in 5% CO_2 at 90% humidity.

MBCs reprogramming was performed by electroporation with the reprogramming episome set [pCE-hUL, pCE-hSK, pCE-hOCT3/4, pCE-mp53DD, pCE-GFP, pCXB-EBNA-1 (Addgene; #41855-58, #41813-14)] using Neon Transfection System (Thermo Fisher Scientific) as described in [32]. Primary iPSC colonies were transferred on a feeder layer (mitotically inactive mouse embryonic fibroblasts) or hESC-qualified matrix (Matrigel®-ESQ; Corning, USA) on days 20-30 of reprogramming. Feeder-dependent iPSCs were cultured according to the published protocol [33]; xeno-free iPSCs grown on matrix were maintained in E8 media (Thermo Fisher Scientific).

***In vitro* spontaneous differentiation.** The cells were seeded in cultural dishes, grown up to 85-90% confluency, and then detached from the surface by incubation with Collagenase IV (Sigma-Aldrich, USA) for 20-30 min at 37°C. Cell aggregates were transferred to a cultural dish coated with 1% agarose in order to form embryoid bodies (EBs). EBs were maintained in the growth media without basic growth factor in agarose-coated dishes for 2 weeks and then for 2 more weeks on a gelatin-coated surface.

Immunostaining. The cells were washed twice with PBS, fixed with 4% formamide solution for 10 min at room temperature, washed twice with PBS for 15 min, permeabilized with 0.5% Triton X-100 for 30 min at room temperature, and washed with PBS twice for 15 min. The cells were then incubated with the blocking solution (bovine serum albumin, 10 mg/ml) for 30 min, incubated with specific primary antibody overnight at 4°C, washed with PBS twice for 15 min, and incubated with the secondary antibody for 1.5-2 h at room temperature with subsequent washing with PBS (twice for 15 min at room temperature). Cell nuclei visualized with 4′,6-diamidino-2-phenylindole (DAPI, 1 μg/ml solution in PBS; Sigma-Aldrich), and the cells were analyzed using a Nikon Eclipse Ti-E fluorescent microscope (Nikon, Japan).

RNA isolation, cDNA synthesis, and qPCR. Total RNA was isolated from the cells using TRIzol reagent (Thermo Fisher Scientific) and treated with DNA-free™ DNA removal kit (Ambion, USA) according to the manufacturer's instructions. cDNA was synthesized with SuperScript II reverse transcriptase kit (Thermo Fisher

Scientific). Expression of pluripotency markers was evaluated by RT-PCR according to the protocols published in [1].

Karyotyping. Karyotype analysis of iPSCs was performed as described in [34].

Electroporation of iPSCs. Feeder-dependent cells were transferred on the matrix and cultured for 1-2 passages prior to electroporation. The cells were seeded at 1 : 3 to 1 : 4 dilution 24 h before electroporation. On the day of electroporation, the cells were dissociated from the plate with TrypLE (Thermo Fisher Scientific), centrifuged for 5 min at 200*g*, and resuspended in R buffer (Neon Transfection System 100 µl kit; Thermo Fisher Scientific) to the concentration of $0.5 \cdot 10^7$ cells/ml. For one reaction (100 µl), 2 µg of pX458-AAVS1 and 3 µg of AAVS-Neo-M2rtTA (Addgene; #60843 [35]) were used. The following settings for electroporation were used: 1100 V, 30 ms, 1 pulse. After electroporation, the cells were transferred to the cultural dish containing warm growth media supplemented with 10 ng/ml Y-27632 (Sigma-Aldrich) inhibitor of Rho-associated protein kinase. The medium was replaced with the fresh one supplemented with Y-27632 4 h after electroporation.

iPSC subclone selection on selective medium. For subclone selection, the growth media was supplemented with neomycin sulfate (Thermo Fisher Scientific). Neomycin concentration was determined for each cell line by titration. The cells were maintained in the selective media for 5 days; the colonies that survived selection were transferred into separate cultural dishes for further culturing and analysis.

Subclone analysis and screening. To identify subclones with target CRISPR-mediated transgene insertions, genomic DNA was isolated from the cells with Quick Extract DNA Extraction Solution (Epicentre, USA) according to the manufacturer's instructions and stored at −20°C. PCR was performed using Biomaster HS-Taq PCR-Color 2× mix (Biolabmix, Russia) and primers listed in the Table 2.

Table 2. Primers used to verify transgene insertion

Primer	Sequence, 5′–3′	Comment
AAVS1_WT-F	CTCTGGCTCCATCGTAAGCAA	product length, 555 bp; WT *AAVS1* allele amplification
AAVS1_WT-R	CCCAAAGTACCCCGTCTCCC	product length, 555 bp; WT *AAVS1* allele amplification
HA_L-OUT	CCGGACCACTTTGAGCTCTAC	annealing outside left homology arm
Neo_in-R	GCCCAGTCATAGCCGAATAG	+ HA_L-OUT, product length, 1042 bp; for insert position analysis + HA_L-F1, product length, 461 bp; insert verification
HA_L-F1	CTGTGGATTCGGGTCACCTC	annealing inside left homology arm
M13-R	CAGGAAACAGCTATGAC	+ Neo_in-R, product length, 1063 bp; additional insert verification

Table 3. Genetically-encoded biosensors and their application

Name	Target	Field of study
pXBP1-TagRFP-ERSS	XBP1, ER stress indicator	neurodegenerative diseases [28], Crohn's disease [27]
pCyto-Grx1-roGFP2-donor, pMito-Grx1-roGFP2-donor	roGFP2-Grx1, glutathione redox state sensor	cancer, diabetes [36]
pCyto-roGFP2-Orp1-donor, pMito-roGFP2-Orp1-donor	roGFP2-Orp1, H_2O_2 redox activity sensor	chronic inflammatory diseases [37]
pCasper3-BG-donor, pCasper3-GR-donor	caspase 3, apoptosis	apoptosis in neurodegeneration
pAAVS-TRE-CMV-GCaMP6f/m/s	Ca^{2+}-dependent hyperexcitability	excitability of the specific cells [29]

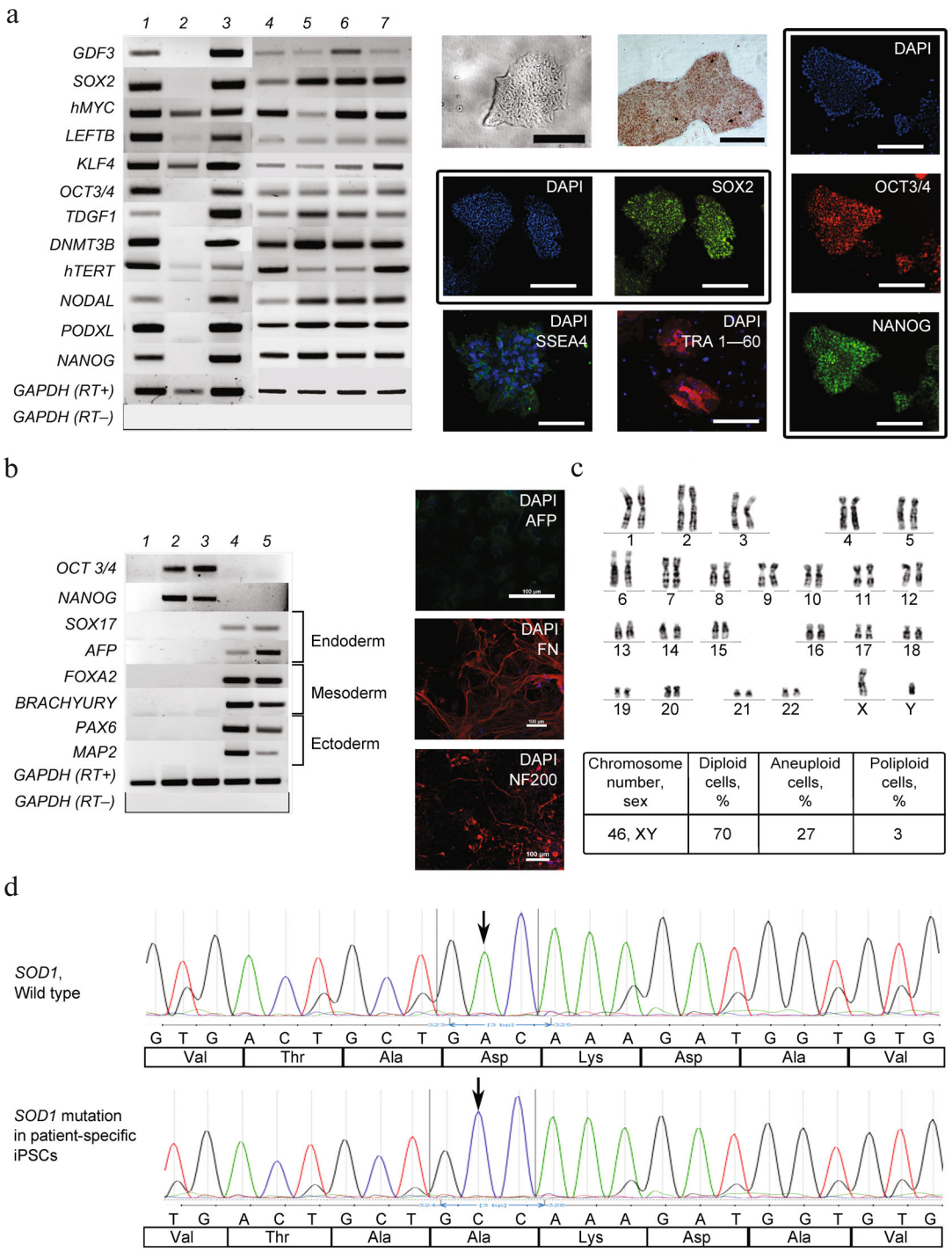

Fig. 1. Characterization of patient-specific iPSCs. a) Left panel, RT-PCR analysis of pluripotency marker expression: *1*) positive control (cDNA of HUES9 embryonic stem cells); *2*) negative control (cDNA of MBCs); *3-7*) iPSC lines 1M_iALS, 2g_iALS, 1g_iALS, 2M_iALS, and 3M_iALS, respectively. Expression of transcription factors (*SOX2*, *hMYC*, *KLF4*, *OCT 3/4*, *NANOG*) and regulatory proteins (*GDF3*, *LEFTB*, *TDGF1*, *DNMT3B*, *hTERT*, *NODAL*, *PODXL*) is shown; *GAPDH* (*RT+*), positive control of reverse transcription reaction; *GAPDH* (*RT–*), control for genomic DNA contamination. Right panel, morphology of iPSC colonies, endogenic alkaline phosphatase expression, immunostaining of 1M_iALS iPSC colonies for transcriptional factors SOX2, OCT3/4, NANOG and membrane antigens SSEA4 and TRA-1-60. Cell nuclei are visualized with DAPI. Magnification, 10×; scale bar, 250 μm. b) *In vitro* spontaneous differentiation. RT-PCR analysis of expression of ectoderm (*PAX6*, *MAP2*), mesoderm (*FOXA2*, *BRACHYURY*), and endoderm (*AFP*, *SOX17*) markers: *1*) cDNA of MBCs; *2*, *3*) cDNA of iPSC lines 1M_iALS and 3M_iALS, respectively; *4*, *5*) cDNA of embryoid bodies derived from 1M_iALS and 3M_iALS, respectively. Immunostaining for the ectoderm (neurofilament 200, NF200), mesoderm (fibronectin, FN), and endoderm (α-fetoprotein, AFP) markers. Cell nuclei are visualized with DAPI. Scale bar, 100 μm. c) Karyotype of the 2M_iALS iPSCs. d) Partial sequence of the *SOD1* gene exon 4; single nucleotide substitution is marked by an arrow.

RESULTS

Generation of donor plasmids for insertion of biosensor sequences in the *AAVS1* safe harbor site. A series of donor plasmids for the CRISPR-mediated insertion of biosensor sequences in the *AAVS1* locus were created: pXBP1-TagRFP-ERSS, pCyto-Grx1-roGFP2-donor, pMito-Grx1-roGFP2-donor, pCyto-roGFP2-Orp1-donor, pMito-roGFP2-Orp1-donor, pCasper3-BG-donor, pCasper3-GR-donor, pAAVS-TRE-CMV-GCaMP6f/m/s. Each donor plasmid contained the biosensor sequence, homology arms to the *AAVS1* locus required for the transgene insertion by the homology-directed repair mechanism, and puromycin resistance sequence for clone selection (Table 3).

Generation and characterization of patient-specific iPSC. Thirteen primary iPSC colonies were obtained by MBC reprogramming: 11 feeder-dependent lines and 2 xeno-free lines (i.e., grown in the medium containing no components derived from animals). Generated iPSCs displayed high nucleus-to-cytoplasm ratio and embryonic stem cell-like morphology of the colonies and expressed endogenous alkaline phosphatase and pluripotency markers genes (Fig. 1a). *In vitro* spontaneous differentiation of these cells resulted in the formation of ecto-, meso- and endoderm derivatives (Fig. 1b). Therefore, iPSCs obtained from the patient's MBCs were pluripotent and able to produce derivatives of three germ layer *in vitro*. Karyotype analysis of iPSCs on passage 10 revealed no significant chromosomal aberrations (Fig. 1c). The cells retained the donor genotype and had a single nucleotide substitution in exon 4 of the *SOD1* gene resulting in the D90A mutation in the SOD1 protein (Fig. 1d).

CRISPR/Cas9-mediated insertion of doxycycline-dependent transactivator sequence in the *AAVS1* locus. Both patient-specific iPSC line 1M_iALS and control healthy iPSC line iMA_1L were used in the experiment. Doxycycline-dependent transactivator sequence was inserted in the *AAVS1* loci of these cells by homologous recombination initiated by the CRISPR/Cas9-induced double-strand break. As a result of electroporation and subsequent selection, 23 to 32 neomycin-resistant subclones were obtained. Sequencing of these subclones confirmed that all of them contained transactivator sequence in the *AAVS1* locus. However, to be used for further introduction of biosensor sequences, the cells should have unchanged protospacer for CRISPR/Cas9 in the *AAVS1* locus on homologous chromosome. Sequencing of the protospacer-containing fragment of the *AAVS1* locus revealed six 1M_iALS subclones and seven iMA_1L subclones that satisfied this condition and can be used for subsequent CRISPR/Cas9-mediated insertion of biosensor sequences in the remaining *AAVS1* locus.

Screening of cell lines for additional off-target transactivator insertions. Since plasmids are prone to random integration into genome, it was necessary to confirm the absence of additional off-target insertions of the donor plasmids that could potentially impact normal cell functioning and/or disease phenotype. Using primers designed for amplification of the nonintegrating fragment of the donor plasmid, we demonstrated by PCR analysis that subclones 4, 11, 3.2, and 6.2 of the iMA_1L cell line and subclones 7, 12, 16, and 27 of the 1M_iALS cell line carried additional copies of the plasmid in the genome, while subclones 17, 19.2, and 24.2 of the iMA_1L cell line and subclones 2 and 17 of the 1M_iALS cell line did

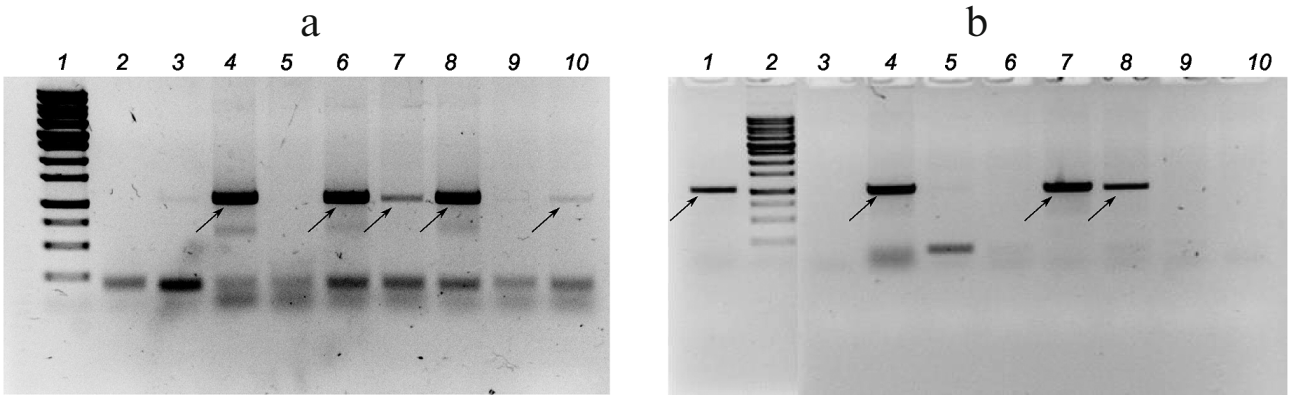

Fig. 2. PCR analysis of subclones for additional random plasmid integration. a) Subclones derived from the 1M_iALS iPSC line: *1*) DNA size ladder (Sky-High; Biolabmix, Russia); *2*) negative control, H_2O (no DNA template); *3*) negative control (genomic DNA from 1M_iALS); *4*) positive control (donor plasmid DNA); *5-10*) 1M_iALS subclones #2, #7, #12, #16, #17, and #27, respectively, containing insertion in the *AAVS1* locus. b) Subclones derived from the iMA_1L iPSC line: *1*) positive control (donor plasmid DNA); *2*) DNA size ladder (Sky-High); *3*) negative control (genomic DNA from iMA_1L); *4-10*) iMA_1L subclones #4, #11, #17, #3.2, #6.2, and #24.2, respectively, containing insertion in the *AAVS1* locus. Target PCR product (1063 bp) is marked by the arrow.

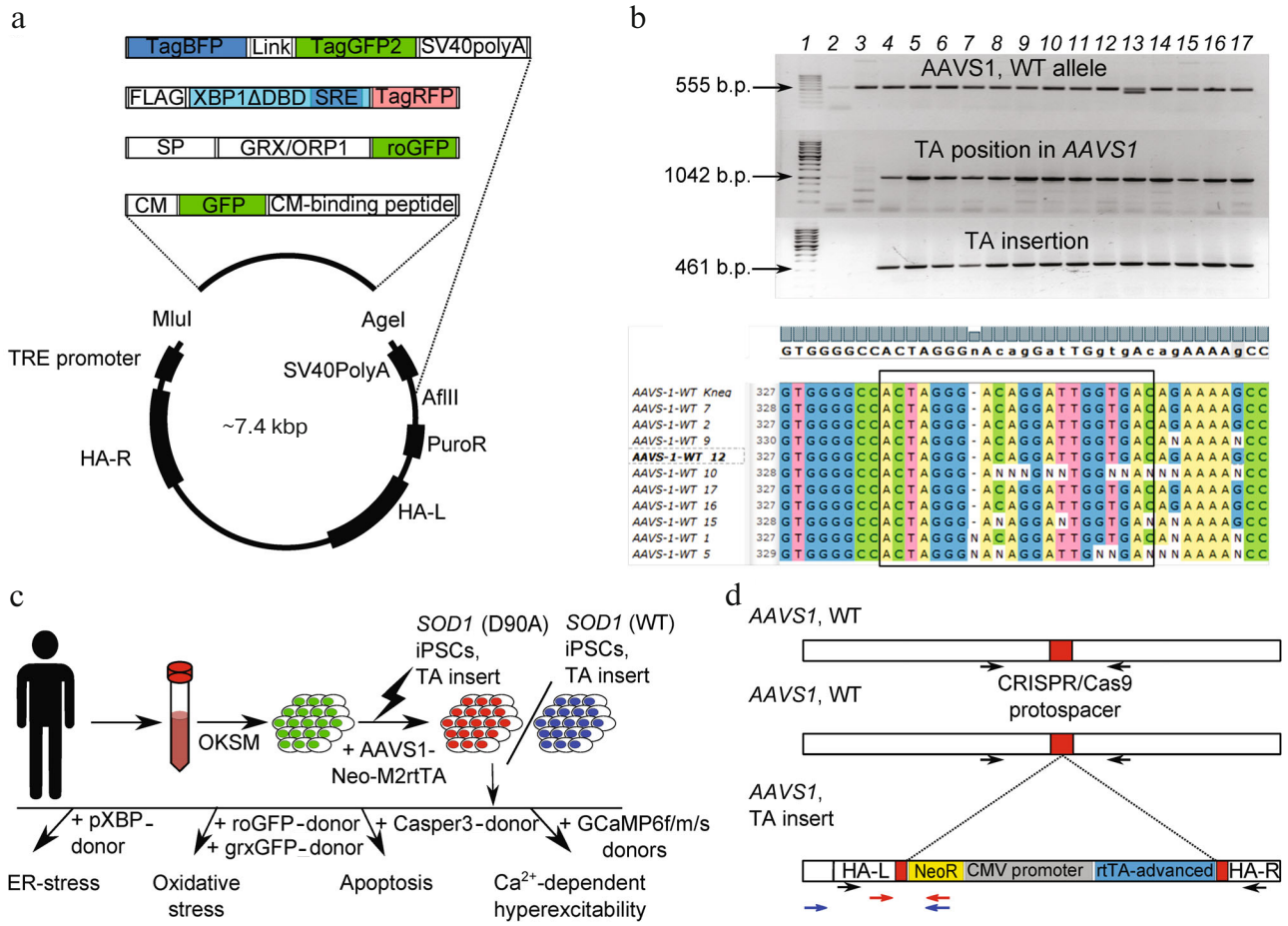

Fig. 3. Development of the universal cell-based platform for neurodegeneration studies. a) Scheme for the donor plasmid construction. The fragment common for all donor plasmids contains the *AAVS1* homology arms (HA-R, HA-L), TRE (tetracycline responsive element) promoter, puromycin-resistance sequence. Plasmid fragments containing functional elements of the biosensors are shown separately: XBP1ΔDBD, fragment of the *XBP1* gene; SRE, stress responsive element; SP, signal peptide from ATP synthase subunit 9 (in pMito-Grx1-roGFP2-donor and pMito-roGFP2-Orp1-donor); Link, caspase 3 hydrolysis site; CM, calmodulin. b) PCR analysis for insert verification in the *AAVS1* site in 1M_iALS subclones: *1*) DNA size ladder (Sky-High; Biolabmix, Russia); *2*) negative control, H_2O (no DNA template); *3*) negative control (genomic DNA from 1M_iALS); *4-17*) 1M_iALS subclones. Partial sequence of the *AAVS1* locus without transactivator insertion in 1M_iALS subclones. CRISPR/Cas9 protospacer sequence is framed. In some subclones, the protospacer sequence is disrupted as a result of double-strand break repair by non-homology directed repair mechanism. WT, wild type; TA, transactivator for doxycycline-dependent expression. c) Strategy for the development of the cell-based platform and its application in ALS studies. OKSM, reprogramming factors OCT3/4, KLF4, SOX2, and MYC. d) *AAVS1* locus structure in 1M_iALS subclones. Transactivator sequence insertion and disrupted CRISPR/Cas9 protospacer on one of the chromosomes and intact CRISPR/Cas9 protospacer on the homologous chromosome are shown. Arrows indicate primers used for the WT *AAVS1* locus amplification (black), transactivator insert verification (red), and verification of transactivator position in the *AAVS1* locus (blue). *NeoR*, neomycin-resistant sequence gene; *rtTA-advanced*, transactivator for doxycycline-dependent expression.

not contained additional insertions of the donor plasmid in the genome (Fig. 2, a and b).

DISCUSSION

It has been shown earlier in different model systems that ER stress, oxidative stress, apoptosis, and neuronal hyperexcitability play a pivotal role in ALS pathophysiology. However, due to the absence of reliable research methods, it is still difficult to establish contribution of each component to the disease onset and progress. Here, we report generation of plasmid constructs encoding biosensors designed to monitor certain pathological processes in living cells (Table 3). The method described in this paper is universal and allows to obtain a wide variety of donor plasmids by replacing biosensor sequences in the same plasmid (Fig. 3a). The sequence of the donor plasmid is organized in a way that the protospacer for CRISPR/Cas9 is absent in the integrating part of the plasmid, thus preventing hydrolysis of both the donor plasmid itself and the corresponding insert in the *AAVS1* locus.

Biosensors encoded in the constructed donor plasmids can be used for studying pathological processes associated with motor neuron death in cell-based ALS models. However, since ALS-associated neurodegeneration is a complex process involving disruption of several different cellular mechanisms, it is convenient to have a universal platform that can be used for the generation of transgenic cell lines with different biosensors (Fig. 3, b and c). In this work, we described two transgenic iPSC lines that have the transactivator sequence inserted in the *AAVS1* site. One of them was generated from MBCs of the ALS patient carrying D90A substitution in *SOD1*. The other was an earlier obtained cell line from a healthy donor (Fig. 3d). Generated iPSCs demonstrated embryonic cell-like morphology, expressed major pluripotency markers, and produced derivatives of three germ layers as a result of *in vitro* spontaneous differentiation. They had a stable number of chromosomes; diploid cells dominated in the culture, except occasional appearance of aneuploid cells that was associated with the sample preparation process.

Transgenic lines with inserted doxycycline-dependent transactivator sequence were generated from the patient-specific iPSCs (1M_iALS) and healthy control iPSCs (iMA_1L) via CRISPR/Cas9-mediated introduction of a double-strand break in the *AAVS1* locus, one of the "safe harbor" loci that can be genetically manipulated without harmful consequences for the cell [36]. Several neomycin-resistant subclones of 1M_iALS and iMA_1L lines were obtained; some of these clones had intact CRISPR/Cas9 protospacer in *AAVS1* locus on homologous chromosome, which is essential for subsequent insertion of the biosensor sequences.

Subclones with no additional off-target integration of the transactivator sequence were identified by PCR. Since the fragment of the donor plasmid that integrated into the *AAVS1* site included transactivator and neomycin resistance sequences only, no other fragments of the donor plasmid should be present in the cells after a certain amount of time required for complete plasmid elimination. We used 6 μg (963.3 fmol) of the AAVS-Neo-M2rtTA donor plasmid for transfection of 10^6 cells. Provided that all plasmid copies (10,080 bp) entered the cells, $5.8 \cdot 10^5$ [$(963.3 \cdot 10^{-15}$ mol $\times 6.022 \times 10^{23})/(1 \times 10^6)$] plasmid copies were introduced into each cell. Since it is impossible to determine the actual number of plasmids transfected into the cell, we used the number $5.8 \cdot 10^5$ plasmid copies per cell for the simplicity of the following calculations. Theoretically, the number of plasmid copies is reduced by 2 every cell cycle; hence, complete elimination of the plasmid occurs after $\log_2 5.8 \times 10^5 = 19.146$ (~20) cell divisions, or cell culturing for ~2 weeks [37]. PCR analysis revealed that two 1M-iALS subclones and three 1MA_1L subclones carried no additional transgene inserts.

In conclusion, here we report generation of the universal cell-based platform including two iPSC lines derived from the ALS patient with ALS-associated mutation in the *SOD1* gene and healthy donor and a series of biosensor-encoding donor plasmids. The cell lines described in this paper can be used for the generation of new cell lines by a one-step insertion of a biosensor sequence into the *AAVS1* locus. The use of biosensors allows to investigate precise mechanisms of impairments in diseased motor neurons by detecting and evaluating certain pathological processes, which might also open new prospects for development of new therapeutic approaches and drug testing.

Acknowledgements

The studies were implemented using equipment of the Center for Genetic Resources of Laboratory Animals (Institute of Cytology and Genetics, Siberian Branch of the Russian Academy of Sciences) supported by the Ministry of Education and Science of Russia (project RFMEFI62117X0015).

Funding

This work was supported by the Russian Foundation for Basic Research (project 18-34-00440) and Basic Research Program of the Presidium of the Russian Academy of Sciences "Basic research for biomedical technologies" (project 0324-2018-0042).

Conflict of Interest

Authors declare no conflict of interest.

Ethical Standards

All procedures involving human subjects were performed according to the ethical standards of the Declaration of Helsinki of 1964 and its subsequent changes or comparable ethical norms. Every person involved in the study gave voluntary informed consent.

REFERENCES

1. Takahashi, K., and Yamanaka, S. (2006) Induction of pluripotent stem cells from mouse embryonic and adult fibroblast cultures by defined factors, *Cell*, **126**, 663-676.
2. Yu, J., Vodyanik, M. A., Smuga-Otto, K., Antosiewicz-Bourget, J., Frane, J. L., Tian, S., Nie, J., Jonsdottir, G. A., Ruotti, V., Stewart, R., Slukvin, I. I., and Thomson, J. A. (2007) Induced pluripotent stem cell lines derived from human somatic cells, *Science*, **318**, 1917-1920.

3. Wiethoff, S., Arber, C., Li, A., Wray, S., Houlden, H., and Patani, R. (2015) Using human induced pluripotent stem cells to model cerebellar disease: hope and hype, *J. Neurogenet.*, **29**, 95-102.
4. Ghaffari, L. T., Starr, A., Nelson, A. T., and Sattler, R. (2018) Representing diversity in the dish: using patient-derived *in vitro* models to recreate the heterogeneity of neurological disease, *Front. Neurosci.*, **12**, 1-18.
5. Israel, M. A., Yuan, S. H., Bardy, C., Reyna, S. M., Mu, Y., Herrera, C., Hefferan, M. P., Van Gorp, S., Nazor, K. L., Boscolo, F. S., Carson, C. T., Laurent, L. C., Marsala, M., Gage, F. H., Remes, A. M., Koo, E. H., and Goldstein, L. S. B. (2012) Probing sporadic and familial Alzheimer's disease using induced pluripotent stem cells, *Nature*, **482**, 216-220.
6. Zou, J., Mali, P., Huang, X., Dowey, S. N., and Cheng, L. (2011) Site-specific gene correction of a point mutation in human iPS cells derived from an adult patient with sickle cell disease, *Blood*, **118**, 4599-4608.
7. Ananiev, G., Williams, E. C., Li, H., and Chang, Q. (2011) Isogenic pairs of wild type and mutant induced pluripotent stem cell (iPSC) lines from Rett syndrome patients as *in vitro* disease model, *PLoS One*, **6**, e25255.
8. Dimos, J. T., Rodolfa, K. T., Niakan, K. K., Weisenthal, L. M., Mitsumoto, H., Chung, W., Croft, G. F., Saphier, G., Leibel, R., Goland, R., Wichterle, H., Henderson, C. E., and Eggan, K. (2008) Induced pluripotent stem cells generated from patients with ALS can be differentiated into motor neurons, *Science*, **321**, 1218-1221.
9. Alves, C. J., Dariolli, R., Jorge, F. M., Monteiro, M. R., Maximino, J. R., Martins, R. S., Strauss, B. E., Krieger, J. E., Callegaro, D., and Chadi, G. (2015) Gene expression profiling for human iPS-derived motor neurons from sporadic ALS patients reveals a strong association between mitochondrial functions and neurodegeneration, *Front. Cell. Neurosci.*, **9**, 289.
10. Wijesekera, L. C., and Leigh, P. N. (2009) Amyotrophic lateral sclerosis, *Orphanet J. Rare Dis.*, **4**, 3.
11. Brites, D., and Vaz, A. R. (2014) Microglia centered pathogenesis in ALS: insights in cell interconnectivity, *Front. Cell. Neurosci.*, **8**, 117.
12. Celeste, D. B., and Miller, M. S. (2018) Reviewing the evidence for viruses as environmental risk factors for ALS: a new perspective, *Cytokine*, **108**, 173-178.
13. Oskarsson, B., Horton, D. K., and Mitsumoto, H. (2015) Potential environmental factors in amyotrophic lateral sclerosis, *Neurol. Clin.*, **33**, 877-888.
14. Ajroud-Driss, S., and Siddique, T. (2014) Sporadic and hereditary amyotrophic lateral sclerosis (ALS), *Biochim. Biophys. Acta*, **1852**, 679-684.
15. Abel, O., Powell, J. F., Andersen, P. M., and Al-Chalabi, A. (2012) ALSoD: a user-friendly online bioinformatics tool for amyotrophic lateral sclerosis genetics, *Hum. Mutat.*, **33**, 1345-1351.
16. Doi, H., Koyano, S., Suzuki, Y., Nukina, N., and Kuroiwa, Y. (2010) The RNA-binding protein FUS/TLS is a common aggregate-interacting protein in polyglutamine diseases, *Neurosci. Res.*, **66**, 131-133.
17. Cortese, A., Plagnol, V., Brady, S., Simone, R., Lashley, T., Acevedo-Arozena, A., de Silva, R., Greensmith, L., Holton, J., Hanna, M. G., Fisher, E. M. C., and Fratta, P. (2014) Widespread RNA metabolism impairment in sporadic inclusion body myositis TDP43-proteinopathy, *Neurobiol. Aging*, **35**, 1491-1498.
18. Watson, M. R., Lagow, R. D., Xu, K., Zhang, B., and Bonini, N. M. (2008) A drosophila model for amyotrophic lateral sclerosis reveals motor neuron damage by human SOD1, *J. Biol. Chem.*, **283**, 24972-24981.
19. Sakowski, S. A., Lunn, J., Busta, A. S., Oh, S., Zamora-Berridi, G., Palmer, M., Rosenberg, A. A., Philip, S. G., Dowling, J. J., and Feldman, E. L. (2012) Neuromuscular effects of G93A-SOD1 expression in zebrafish, *Mol. Neurodegener.*, **7**, 44.
20. Allen, S. P., Rajan, S., Duffy, L., Mortiboys, H., Higginbottom, A., Grierson, A. J., and Shaw, P. J. (2014) Superoxide dismutase 1 mutation in a cellular model of amyotrophic lateral sclerosis shifts energy generation from oxidative phosphorylation to glycolysis, *Neurobiol. Aging*, **35**, 1499-1509.
21. Richardson, K., Allen, S. P., Mortiboys, H., Grierson, A. J., Wharton, S. B., Ince, P. G., Shaw, P. J., and Heath, P. R. (2013) The effect of SOD1 mutation on cellular bioenergetic profile and viability in response to oxidative stress and influence of mutation-type, *PLoS One*, **8**, e68256.
22. Gutscher, M., Pauleau, A.-L., Marty, L., Brach, T., Wabnitz, G. H., Samstag, Y., Meyer, A. J., and Dick, T. P. (2008) Real-time imaging of the intracellular glutathione redox potential, *Nat. Methods*, **5**, 553-559.
23. Iwawaki, T., Akai, R., Kohno, K., and Miura, M. (2004) A transgenic mouse model for monitoring endoplasmic reticulum stress, *Nat. Med.*, **10**, 98-102.
24. Schwarzlander, M., Dick, T. P., Meyer, A. J., and Morgan, B. (2016) Dissecting redox biology using fluorescent protein sensors, *Antioxid. Redox Signal.*, **24**, 680-712.
25. Esposito, S., Masala, A., Sanna, S., Rassu, M., Pimxayvong, V., Iaccarino, C., and Crosio, C. (2017) Redox-sensitive GFP to monitor oxidative stress in neurodegenerative diseases, *Rev. Neurosci.*, **28**, 133-144.
26. Morgan, B., Sobotta, M. C., and Dick, T. P. (2011) Measuring E(GSH) and H_2O_2 with roGFP2-based redox probes, *Free Radic. Biol. Med.*, **51**, 1943-1951.
27. Kaser, A., Lee, A.-H., Franke, A., Glickman, J. N., Zeissig, S., Tilg, H., Nieuwenhuis, E. E. S., Higgins, D. E., Schreiber, S., Glimcher, L. H., and Blumberg, R. S. (2008) XBP1 links ER stress to intestinal inflammation and confers genetic risk for human inflammatory bowel disease, *Cell*, **134**, 743-756.
28. Nishitoh, H., Kadowaki, H., Nagai, A., Maruyama, T., Yokota, T., Fukutomi, H., Noguchi, T., Matsuzawa, A., Takeda, K., and Ichijo, H. (2008) ALS-linked mutant SOD1 induces ER stress- and ASK1-dependent motor neuron death by targeting Derlin-1, *Genes Dev.*, **22**, 1451-1464.
29. Chen, T.-W., Wardill, T. J., Sun, Y., Pulver, S. R., Renninger, S. L., Baohan, A., Schreiter, E. R., Kerr, R. A., Orger, M. B., Jayaraman, V., Looger, L. L., Svoboda, K., and Kim, D. S. (2013) Ultrasensitive fluorescent proteins for imaging neuronal activity, *Nature*, **499**, 295-300.
30. Ran, F. A., Hsu, P. D., Wright, J., Agarwala, V., Scott, D. A., and Zhang, F. (2013) Genome engineering using the CRISPR-Cas9 system, *Nat. Protoc.*, **8**, 2281-2308.
31. Soares, F. A. C., Pedersen, R. A., and Vallier, L. (2015) Generation of human induced pluripotent stem cells from peripheral blood mononuclear cells using Sendai virus, in

Methods in Molecular Biology series, *Induced Pluripotent Stem (iPS) Cells: Methods and Protocols* (Turksen, K., and Nagy, A., eds.) Humana Press, N. Y., pp. 23-31.

32. Okita, K., Yamakawa, T., Matsumura, Y., Sato, Y., Amano, N., Watanabe, A., Goshima, N., and Yamanaka, S. (2013) An efficient nonviral method to generate integration-free human-induced pluripotent stem cells from cord blood and peripheral blood cells, *Stem Cells*, **31**, 458-466.
33. Medvedev, S. P., Grigor'eva, E. V., Shevchenko, A. I., Malakhova, A. A., Dementyeva, E. V., Shilov, A. A., Pokushalov, E. A., Zaidman, A. M., Aleksandrova, M. A., Plotnikov, E. Y., Sukhikh, G. T., and Zakian, S. M. (2011) Human induced pluripotent stem cells derived from fetal neural stem cells successfully undergo directed differentiation into cartilage, *Stem Cells Dev.*, **20**, 1099-1112.
34. Minina, J. M., Borodin, P. M., Searle, J. B., Volobouev, V. T., and Zhdanova, N. S. (2007) Standard DAPI karyotype of the common shrew *Sorex araneus* L. (Soricidae, Eulipotyphla), *Russ. J. Teriol.*, **6**, 3-6.
35. DeKelver, R. C., Choi, V. M., Moehle, E. A., Paschon, D. E., Hockemeyer, D., Meijsing, S. H., Sancak, Y., Cui, X., Steine, E. J., Miller, J. C., Tam, P., Bartsevich, V. V., Meng, X., Rupniewski, I., Gopalan, S. M., Sun, H. C., Pitz, K. J., Rock, J. M., Zhang, L., Davis, G. D., Rebar, E. J., Cheeseman, I. M., Yamamoto, K. R., Sabatini, D. M., Jaenisch, R., Gregory, P. D., and Urnov, F. D. (2010) Functional genomics, proteomics, and regulatory DNA analysis in isogenic settings using zinc finger nuclease-driven transgenesis into a safe harbor locus in the human genome, *Genome Res.*, **20**, 1133-1142.
36. Papapetrou, E. P., and Schambach, A. (2016) Gene insertion into genomic safe harbors for human gene therapy, *Mol. Ther. Am. Soc. Gene Cell Ther.*, **24**, 678-684.
37. Wadkin, L. E., Elliot, L. F., Neganova, I., Parker, N. G., Chichagova, V., Swan, G., Laude, A., Lako, M., and Shukurov, A. (2017) Dynamics of single human embryonic stem cells and their pairs: a quantitative analysis, *Sci. Rep.*, **7**, 570.
38. Gonzalez, F., Zhu, Z., Shi, Z.-D., Lelli, K., Verma, N., Li, Q. V., and Huangfu, D. (2014) An iCRISPR platform for rapid, multiplexable, and inducible genome editing in human pluripotent stem cells, *Cell Stem Cell*, **15**, 215-226.
39. Kleinstiver, B. P., Pattanayak, V., Prew, M. S., Tsai, S. Q., Nguyen, N. T., Zheng, Z., and Joung, J. K. (2016) High-fidelity CRISPR-Cas9 nucleases with no detectable genome-wide off-target effects, *Nature*, **529**, 490-495.
40. Gutscher, M., Sobotta, M. C., Wabnitz, G. H., Ballikaya, S., Meyer, A. J., Samstag, Y., and Dick, T. P. (2009) Proximity-based protein thiol oxidation by H_2O_2-scavenging peroxidases, *J. Biol. Chem.*, **284**, 31532-31540.